Plane Waves on a Periodic Structure of Circular Disks and Their Application to Surface-Wave Antennas*

JOSHUA SHEFER†, SENIOR MEMBER, IRE

Summary—**The structure supporting the surface-wave consists of a row of concentric circular disks embedded in a lossless dielectric medium. Exact solutions for the "dipole mode" (corresponding to the HE_{11} surface-wave mode on a dielectric rod) are set up and an approximation is derived for calculating the propagation constants.**

It is shown experimentally that a pure "dipole mode" can be excited by simple means, and that propagation constants may be controlled over a wide range by varying the geometrical parameters of the periodic structure.

The possible uses as a surface-wave antenna are discussed, and approximate radiation patterns are calculated from the field distribution in the terminal plane.

I. Introduction

SURFACE WAVES[1,2] may be guided by a variety of periodic structures such as corrugated surfaces[3] or structures of conducting cylindrical rods.[4] In this paper a periodic structure of circular conducting disks is investigated. It is shown that, in common with other periodic structures, a superposition of an infinite number of propagating modes can satisfy boundary conditions at the cylindrical interface between the periodic structure and free space. Surfaces of equal phase are perpendicular to the propagation axis z, and phase velocities are smaller than those in an unbounded medium.

A periodic structure of disks may be used as an endfire antenna.[5] The circularly symmetrical modes give zero radiation on the axis of the structure, and therefore attention is focused on the propagation characteristics of the nonsymmetrical dipole mode, with a circular field variation of cos ϕ. This mode yields a maximum of radiated power in the axial direction when used as an antenna. It is shown that the beamwidth decreases as the guided wavelength increases and approaches that of free space, provided the excitation efficiency of the surface wave is kept constant.[6] This, as might be expected, is hardly the case, and for antennas with very loosely bound surface waves the excitation efficiency is probably the dominating factor in its performance.

* Received June 16, 1962; revised manuscript received August 6, 1962. This paper was presented at the Nat'l Electronics Conf., Chicago, Ill., October, 1961. It is based in part upon work done by the author while at London University, England.

† Bell Telephone Laboratories, Inc., Whippany, N. J. Formerly with the Gordon McKay Laboratory of Applied Science, Harvard University, Cambridge, Mass.

[1] H. M. Barlow and A. L. Cullen, "Surface waves," *Proc. IEE*, pt. III, vol. 100, pp. 329–347; November, 1953.

[2] F. J. Zucker, "The guiding and radiation of surface waves," *Proc. Symp. on Modern Advances in Microwave Techniques*, Polytechnic Institute of Brooklyn, Brooklyn, N. Y., 1954.

[3] W. Rotman, "A study of single-surface corrugated guides," Proc. IRE, vol. 39, pp. 952–959; August, 1951.

[4] J. O. Spector, "An investigation of periodic rod structures for Yagi aerials," *Proc. IEE*, vol. 105, pt. B, pp. 38–44; January, 1958.

[5] J. C. Simon and G. Weill, "Un nouveau type d'antenne á rayonnement longitudinal," *Ann. de Radioélectricité*, vol. 8, pp. 183–193; July, 1953.

II. Theoretical Discussion

Consider a periodic line shown in Fig. 1. It consists of an array of infinitely thin circular disks with common axis, which is taken as the z axis of the cylindrical coordinate system ρ, ϕ, z. A periodicity d is assumed along the propagation axis z. The disks of diameter $2a$ are embedded in a dielectric medium of constants ϵ, μ, and the cylindrical sandwich structure is suspended in air.

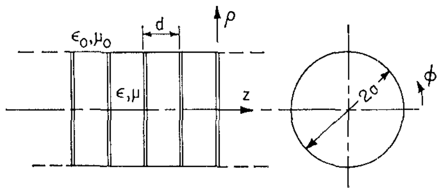

Fig. 1—Periodic structure of disks.

The wave solutions in periodic structures are described by Floquet's Theorem.[7] This solution is given as a sum of "space harmonics" with a z dependence of the mth wave given by

$$e^{-\gamma_m z} \tag{1}$$

where

$$\gamma_m = \gamma_0 + j\frac{2m\pi}{d}$$

$$m = 0; +1; +2; -2 \cdots. \tag{2}$$

The longitudinal components of E and H at $\rho > a$ are given by

$$E_z = \sum_{m=-\infty}^{+\infty} A_m \cos n\phi Z_n(jk_m\rho)e^{-\gamma_m z} \tag{3}$$

$$H_z = \sum_{m=-\infty}^{+\infty} B_m \sin n\phi Z_n(jk_m\rho)e^{-\gamma_m z} \tag{4}$$

[6] J. Brown and J. O. Spector, "The radiating properties of endfire aerials," *Proc. IEE*, vol. 104, Part B, No. 13, pp. 27–34; January, 1957.

[7] J. C. Slater, "Microwave Electronics," D. Van Nostrand Company, Inc., New York, N. Y.; 1950.

with

$$-k_m^2 = \gamma_m^2 + \omega^2\epsilon_0\mu_0 \quad (5)$$

where Z_n is a solution of the Bessel equation of order n.

The present discussion is restricted to the "dipole mode" where $n=1$. Since the region of $\rho=0$ is excluded the Bessel function of the third kind (Hankel function) and order one will be used.

In order to have a plane wave (*i.e.*, a phase change in the z direction only), k_m must be real. Writing λg_m for the guided wavelength of the mth wave and λ_0 for an unbounded wave in free space, we have, from (5),

$$\lambda g_m < \lambda_0. \quad (6)$$

We have, therefore, a superposition of slow waves, with decreasing phase velocities for increasing m. When the periodicity d is small compared with the wavelength of the zeroth space harmonic λg_0, it is seen that

$$k_m \ll k_0, \qquad m \neq 0$$

and, by virtue of (3) and (4), other than zeroth-order space harmonics are found only in close proximity to the periodic guiding structure. Thus, λg_0 is the only wave of practical interest once we are a fraction of a wavelength away from the guiding interface $\rho=a$. This fundamental guided wavelength will be denoted henceforth by λg.

A complete description of the dipole mode fields ($n=1$) outside the disks, where $\rho \geq a$, may be derived from Maxwell's equations, and we obtain

$$E_z = \sum_{m=-\infty}^{+\infty} A_m H_1^{(1)}(jk_m\rho) \cos\phi e^{-\gamma_m z}$$

$$H_z = \sum_{m=-\infty}^{+\infty} B_m H_1^{(1)}(jk_m\rho) \sin\phi e^{-\gamma_m z}$$

$$E_\phi = \sum_{-\infty}^{\infty}\left[-A_m \frac{\gamma_m}{\rho k_m^2} H_1^{(1)}(jk_m\rho) + B_m \frac{\omega\mu_0}{k_m} H_1^{(1)\prime}(jk_m\rho)\right] \cdot \sin\phi e^{-\gamma_m z}$$

$$H_\phi = \sum_{-\infty}^{\infty}\left[-A_m \frac{\omega\epsilon_0}{k_m} H_1^{(1)\prime}(jk_m\rho) + B_m \frac{\gamma_m}{\rho k_m^2} H_1^{(1)}(jk_m\rho)\right] \cdot \cos\phi e^{-\gamma_m z}$$

$$E_\rho = \sum_{-\infty}^{\infty} j\left[A_m \frac{\gamma_m}{k_m} H_1^{(1)\prime}(jk_m\rho) + B_m \frac{\omega\mu_0}{\rho k_m^2} H_1^{(1)}(jk_m\rho)\right] \cdot \cos\phi e^{-\gamma_m z}$$

$$H_\rho = \sum_{-\infty}^{\infty} j\left[A_m \frac{\omega\epsilon_0}{\rho k_m^2} H_1^{(1)}(jk_m\rho) + B_m \frac{\gamma_m}{k_m} H_1^{(1)\prime}(jk_m\rho)\right] \cdot \sin\phi e^{-\gamma_m z} \quad (7)$$

where

$$\gamma_m = \gamma_0 + j\frac{2\pi m}{d}$$

$$-k_m^2 = \gamma_m^2 + \omega^2\epsilon_0\mu_0$$

and A_m, B_m denote amplitudes of electric and magnetic fields, respectively. The time factor $e^{j\omega t}$ will be omitted throughout.

In the spaces between disks when $\rho < a$, we assume cylindrical waves supported by a parallel-plate radial waveguide. A set of TM and TE waves may be derived from

$$E_{zn} = C_n J_1(h_n\rho) \cos\phi \cos\frac{n\pi}{d} z \qquad n = 0, 1, 2, \cdots$$

and

$$H_{zn} = D_n J_1(h_n\rho) \sin\phi \sin\frac{n\pi}{d} z \qquad n = 1, 2, \cdots$$

with

$$h_n^2 = \omega^2\epsilon\mu - \left(\frac{n\pi}{d}\right)^2.$$

A complete set of radial waveguide fields is thus given by

$$E_z = \sum_{n=0}^{\infty} C_n J_1(h_n\rho) \cos\phi \cos\frac{n\pi}{d} z$$

$$H_z = \sum_{n=1}^{\infty} D_n J_1(h_n\rho) \sin\phi \sin\frac{n\pi}{d} z$$

$$E_\phi = \sum_{1}^{\infty}\left[C_n \frac{n\pi}{\rho h_n^2 d} J_1(h_n\rho) + D_n \frac{j\omega\mu}{h_n} J_1'(h_n\rho)\right] \cdot \sin\phi \sin\frac{n\pi}{d} z$$

$$H_\phi = \sum_{0}^{\infty}\left[-C_n \frac{j\omega\epsilon}{h_n} J_1'(h_n\rho) + D_n \frac{n\pi}{\rho h_n^2 d} J_1(h_n\rho)\right] \cdot \cos\phi \cos\frac{n\pi}{d} z$$

$$E_\rho = \sum_{1}^{\infty} -\left[C_n \frac{n\pi}{h_n d} J_1'(h_n\rho) + D_n \frac{j\omega\mu}{\rho h_n^2} J_1(h_n\rho)\right] \cdot \cos\phi \sin\frac{n\pi}{d} z$$

$$H_\rho = \sum_{0}^{\infty}\left[-C_n \frac{j\omega\epsilon}{\rho h_n^2} J_1(h_n\rho) + D_n \frac{n\pi}{d h_n} J_1'(h_n\rho)\right] \cdot \sin\phi \cos\frac{n\pi}{d} z. \quad (8)$$

Boundary conditions require that tangential components of electric and magnetic fields (E_ϕ, H_ϕ, E_z, H_z) be continuous at $\rho = a$. Thus from (7) and (8) we have,

$$\sum_{-\infty}^{\infty} A_m H_1(jk_m a) e^{-\gamma_m z} = \sum_{0}^{\infty} C_n J_1(h_n a) \cos\frac{n\pi}{d} z$$

$$\sum_{-\infty}^{\infty} B_m H_1(jk_m a) e^{-\gamma_m z} = \sum_{1}^{\infty} D_n J_1(h_n a) \sin\frac{n\pi}{d} z$$

$$\sum_{-\infty}^{\infty}\left[\frac{-A_m\gamma_m}{ak_m^2} H_1(jk_m a) + \frac{B_m\omega\mu_0}{k_m} H_1'(jk_m a)\right] e^{-\gamma_m z}$$

$$= \sum_{1}^{\infty}\left[\frac{n\pi}{ah_n^2 d} C_n J_1(h_n a) + \frac{j\omega\mu}{h_n} D_n J_1'(h_n a)\right]\sin\frac{n\pi}{d} z$$

$$\sum_{-\infty}^{\infty}\left[\frac{-A_m\omega\epsilon_0}{k_m} H_1'(jk_m a) + \frac{B_m\gamma_m}{ak_m^2} H_1(jk_m a)\right] e^{-\gamma_m z}$$

$$= \sum_{0}^{\infty}\left[\frac{-j\omega\epsilon}{h_n} C_n J_1'(h_n a) + \frac{n\pi}{ah_n^2 d} D_n J_1(h_n a)\right]\cos\frac{n\pi}{d} z. \quad (9)$$

We now multiply the first and fourth equations of (9) by cos $(n\pi/d)z$, the second and third by sin $(n\pi/d)z$, and integrate from $z=0$ to $z=d$. On eliminating C_n and D_n between the four sets of equations, we obtain

$$\sum_{m=-\infty}^{\infty} \frac{\gamma_m A_m}{\gamma_m^2 + \left(\frac{n\pi}{d}\right)^2}\left[\frac{1}{k_m^2} + \frac{1}{h_n^2}\right]$$

$$= a\omega\mu_0 \sum_{m=-\infty}^{\infty} \frac{B_m}{\gamma_m^2 + \left(\frac{n\pi}{d}\right)^2}\left[\frac{H_1'(jk_m a)}{k_m H_1(jk_m a)} - \frac{j\frac{\mu}{\mu_0} J_1'(h_n a)}{h_n J_1(h_n a)}\right]$$

$$n = 1, 2, \cdots \infty \quad (10)$$

$$a\omega\epsilon_0 \sum_{m=-\infty}^{\infty} \frac{\gamma_m A_m}{\gamma_m^2 + \left(\frac{n\pi}{d}\right)^2}\left[\frac{H_1'(jk_m a)}{k_m H_1(jk_m a)} - \frac{j\frac{\epsilon}{\epsilon_0}}{h_n}\frac{J_1'(h_n a)}{J_1(h_n a)}\right]$$

$$= \sum_{m-\infty}^{\infty} \frac{B_m}{\gamma_m^2 + \left(\frac{n\pi}{d}\right)^2}\left[\left(\frac{\gamma_m}{k_m}\right)^2 - \left(\frac{n\pi}{h_n d}\right)^2\right]$$

$$n = 0, 1, 2, \cdots \infty.$$

Writing this set of equations in matrix form,

$$[K]\{A\} = [L]\{B\}$$

$$[M]\{A\} = [N]\{B\} \quad (11)$$

possible propagation constants are given by

$$[M][K]^{-1}[L] - [N] = 0 \quad (12)$$

where each matrix has an infinite number of elements. For the general case, terms are only slowly converging with m, and no exact expression for the γ_m's has been found.

For a closely spaced structure, however, where $d \ll \lambda_g$, an approximate expression has been derived. It can be seen from (10) that higher order terms are very much smaller than those of zeroth order. Taking leading terms and neglecting all others yields

$$\left(\frac{\gamma_0}{ak_0}\right)^2\left[\frac{1}{(ak_0)^2} + \frac{1}{(ah_1)^2}\right]$$

$$= \omega^2\mu_0\epsilon_0\left[f(ak_0) - \frac{\epsilon}{\epsilon_0} g(ah_0)\right]\left[f(ak_0) - \frac{\mu}{\mu_0} g(ah_1)\right] \quad (13)$$

where

$$f(x) = \frac{H_1'(jx)}{xH_1(jx)}$$

$$g(x) = j\frac{J_1'(x)}{xJ_1(x)}.$$

This characteristic equation can now be solved graphically, but the process is still laborious. A further simplification can be achieved by making $2a > d$, which is frequently the case for closely spaced structures, and assuming $\mu = \mu_0$. Eq. (13) then reduces to

$$\left[\frac{\gamma_0}{(ak_0)^2}\right]^2 = \omega^2\epsilon_0\mu_0\left[f(ak_0) - \frac{\epsilon}{\epsilon_0} g(ah_0)\right] f(ak_0). \quad (14)$$

This approximate solution is independent of the spacing d.

Eq. (14) has been solved graphically using well-known methods for solving transcendental equations. The theoretical results for disks of up to $0.55\lambda_0$ in diameter and $\epsilon/\epsilon_0 = 1$ are shown in Fig. 2. For larger values of $2a$, (14) indicates a series of stop and pass bands. However, near a stop band, as $\lambda_g/\lambda_0 \ll 1$, the condition $\lambda_g \gg d$ is no longer fulfilled and the first-order approximation is no longer valid.

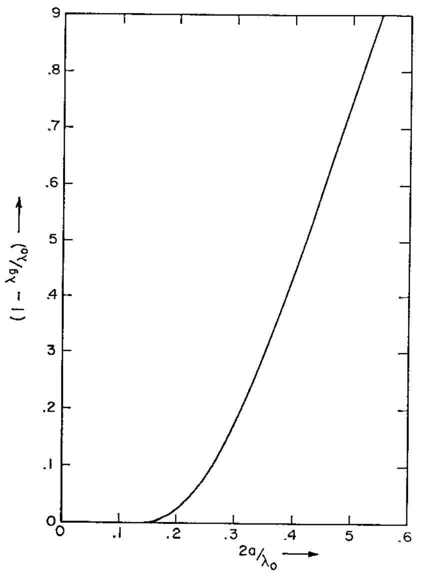

Fig. 2—Guided wavelength λ_g on disk structure, theoretical values. $2a$ is disk diameter.

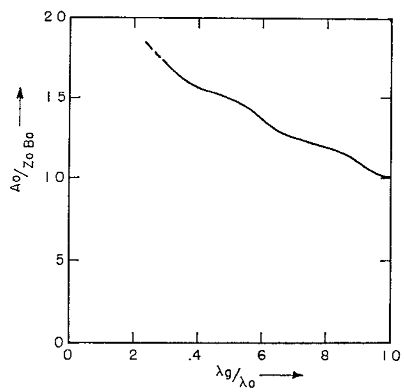

Fig. 3—Theoretical values of impedance ratio A_0/Z_0B_0.

Subject to the same approximation, we may also calculate the wave impedance of the zeroth-order wave. This ratio is given by

$$\frac{A_0}{Z_0B_0} = -j\frac{\lambda_g}{\lambda_0}ak_0\frac{H_1'(jak_0)}{H_1(jak_0)} \tag{15}$$

where

$$Z_0 = \sqrt{\frac{\mu_0}{\epsilon_0}}.$$

As $\lambda_g \to \lambda_0$, this ratio tends to unity. A plot of A_0/Z_0B_0 as a function of λ_g/λ_0 is shown in Fig. 3.

III. Experimental Determination of Phase Velocities

The purpose of the experimental investigation was to establish whether a "dipole mode" surface wave could be supported by the disk structure of Fig. 1, and to measure the propagation constant (or guided wavelength) on structures with different disk diameters and spacings.

Experiments were carried out with the aid of a surface-wave resonator.[1,8] Eight sets of disks were cut from aluminum sheet of 0.01λ thickness. The disk structures were mounted along the center of the resonator. The disks were originally held in a slab of styrofoam. Subsequently it was found that the field on the axis of the structure was not much perturbed by introducing a 2-mm diameter brass supporting rod with 5-mm diameter polystyrene sleeves for spacing. The "dipole mode" was excited by means of an open-end circular waveguide propagating the dominant TE_{11} mode and terminated by a circular opening at the resonator end plate, as shown in Fig. 4. Resonance was obtained by varying the oscillator frequency until a transmission maximum through the resonator was observed by means of a sensitive receiver. (A spectrum analyzer was used for this purpose.) The distance between the resonator end plates was accurately measured and was kept constant throughout the measurements. For every resonance observed, the free-space wavelength was measured by means of an accurate wavemeter, and the guided wavelength was determined by counting the number of minima of the standing wave along the resonator axis. This was done by moving a thin cylindrical obstacle along the disk structure. The condition for resonance was unaffected only when the obstacle was placed at a node of the electric field. By counting the number of power output oscillations at the receiver while the obstacle was traversing the length of the resonator, the number of half-wavelengths was found. The Q factor of the resonator was better than 1000, and an over-all accuracy of 0.05 was estimated for the measured values of λ_g. All measurements were made at wavelengths of approximately 10 cm.

Measured values of guided wavelength as a function of disk diameter, with spacing as parameter, are shown in Fig. 5. It is seen that phase velocities on the disk structure depend to a large extent on the disk diameter and much less on the spacing between disks. This is in agreement with the approximate solution of (14) being independent of d. Theoretical approximate values from (14) are shown for comparison in Fig. 5.

[8] C. H. Chandler, "An investigation of dielectric rod as wave guide," *J. Appl. Phys.*, vol. 20, pp. 1188–1192; December, 1949.

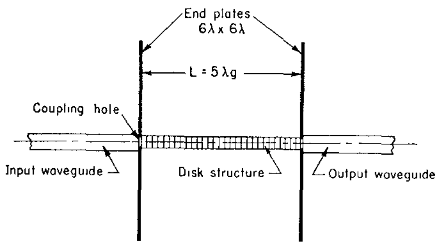

Fig. 4—Surface-wave resonator.

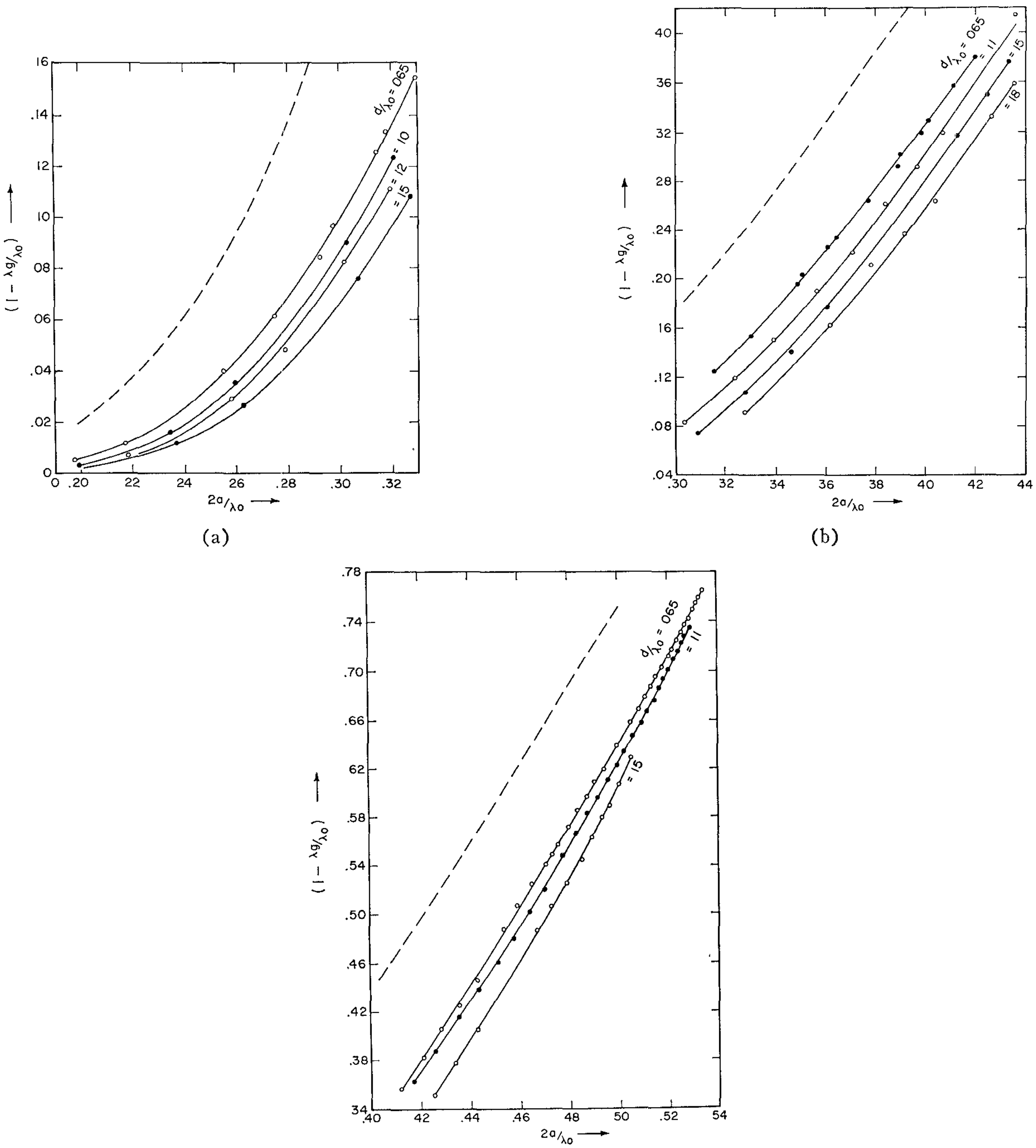

(a) (b)

(c)

2*a*—Disk diameter
d—Disk spacing
– – – Theoretical values for $d \ll \lambda$

Fig. 5—Guided wavelength on disk structure.

IV. Purity of the "Dipole Mode"

As the purity of the "dipole mode" with a circular variation of cos ϕ or sin ϕ is essential when the periodic structure is used as an antenna, it is of some importance to determine experimentally whether any unwanted surface waves were excited.

A perturbation measurement was used, in which a perturbing metallic body was placed in the resonator at points where the fields had to be determined. The relative change of resonance frequency is proportional to the work done when the perturbing body is expanded from zero to a finite volume against the forces of the field.[9] By inserting perturbing bodies of appropriate shape, and given the total energy stored in the resonator, the actual magnitude of the field components can be determined.

In Figs. 6 and 7 the relative change in resonance frequency is given as a function of b/a for prolate and oblate spheroids, normalized with respect to a sphere of radius a, perturbation of which is given by

$$\frac{\delta\omega}{\omega} = \frac{\pi a^3}{A}\left[\frac{\mu_0 H^2}{2} - \epsilon_0 E^2\right] \tag{16}$$

where A is the total energy.[9,10]

It is seen from Figs. 6 and 7 that by using a thin rod-shaped conducting body, the response to the electric field parallel to its axis will be far greater than the contribution of all the other field components, provided that $b/a \ll 1$. By introducing such a thin conducting cylinder in various orientations, the relative magnitudes of the electric fields can be determined. Subsequently it is seen from Fig. 7 that a thin conducting disk with $b/a \ll 1$ will effectively respond to the parallel electric and perpendicular magnetic fields, and since the electric field has already been found by means of the cylinder experiment, the magnetic field can now be determined.

The cylindrical perturbing body used was a copper rod, 0.16λ long and 0.016λ thick ($b/a = 0.1$). It was held in position near the line by embedding it in a slab of polyfoam, which was in turn held in a laterally movable carriage mounted outside the resonator. The copper rod was thus held in position and could be moved in the z direction without introducing any measurable discontinuity into the resonator except the perturbing effect of the rod itself.

Response to magnetic field components was obtained by introducing an aluminum disk with $a = 0.18\lambda$ and $b = 0.0086\lambda$ ($b/a = 0.048$) as perturbing body.

[9] L. C. Maier and J. C. Slater, "Determination of field strength in a linear accelerator cavity," *J. Appl. Phys.*, vol. 23, pp. 78–83; January, 1952.

[10] L. C. Maier, "Field Strength Measurements in Resonant Cavities," M.I.T., Cambridge, Mass., Tech. Rept. No. 143; 1949.

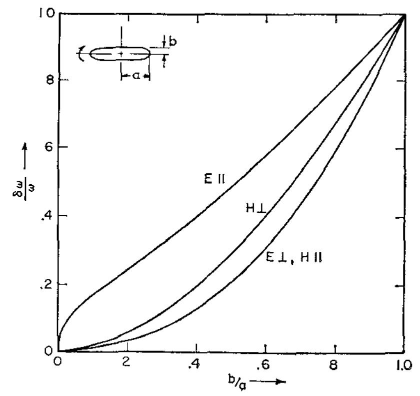

∥ Parallel to a
⊥ Perpendicular to a

Fig. 6—Perturbation due to conducting prolate spheroids, normalized to a sphere of radius a.

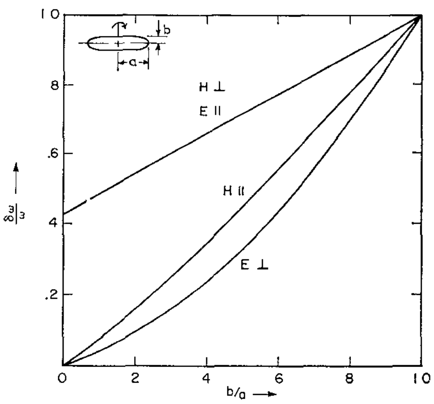

∥ Parallel to a
⊥ Perpendicular to a

Fig. 7—Perturbation due to conducting oblate spheroids, normalized to a sphere of radius a.

A typical set of measurements is shown in Fig. 8. The perturbing body was moved parallel to the axis of the structure until a maximum of frequency shift was observed and thus a maximum of the standing-wave pattern located. The frequency shift was noted and a similar measurement was made in the same plane at right angles. Intermediate readings with $0 < \phi < \pi/2$ were also taken, and values of frequency shifts were found to have a cosine variation with ϕ. For the measurement of E_ϕ the perturbing body was shaped to conform to a circle $\rho = \text{constant}$.

From sets of measured values such as shown in Fig. 8 it was seen that the field configuration was indeed that of a "diple mode." The fact that E_ϕ is zero both at $\phi = 0$ and $\phi = \pi/2$ is in good agreement with the approximate theory given above. The same result is obtained by taking the leading terms in the first equation of (10), together with the expression for E_ϕ at $\rho = a$ from (7), and approximating for $d \ll \lambda_g$ and $d < 2a$.

The ratio E_z/Z_0H_z can also be calculated from the data in Fig. 8. It can readily be shown that

ϕ	POSITION OF PERTURBING BODY RELATIVE TO DISKS	RESPONSE TO	MEASURED PERTURBATION δf Mc/s
0	ρ_1	E_z	-3.4
$\pi/2$		E_z	0
0		E_ρ	-3.5
$\pi/2$		E_ρ	0
0		E_ϕ	0
$\pi/2$		E_ϕ	0
$\pi/2$	ρ_2	H_z	0.5
0		H_z	0
$\pi/2$		H_ρ	3.75
0		H_ρ	0.2

Fig. 8—Results of perturbation experiment.

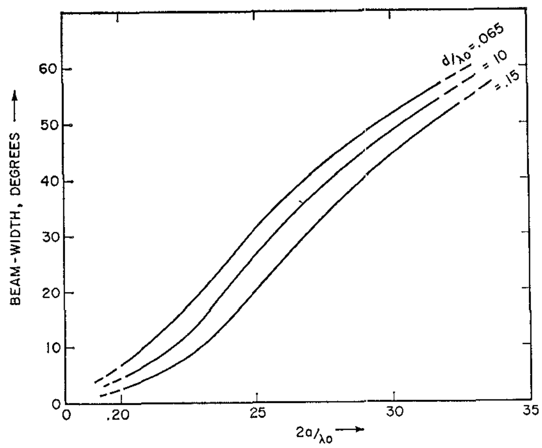

Fig. 9—Theoretical dependence of half-amplitude beamwidth on diameter $2a$ and spacing d of disk structure antenna.

$$\left(\frac{E_z}{Z_0 H_z}\right)_{\rho=\rho_1} = -\alpha\left[\frac{(\delta f_{E_z})_{\rho=\rho_1}}{(\delta f_{H_z})_{\rho=\rho_2}}\right]^{1/2} \frac{H_1(jk_0\rho_2)}{H_1(jk_0\rho_1)}, \tag{17}$$

where

$(\delta f_{E_z})_{\rho=\rho_1}$ = frequency shift for conducting rod measuring E_z at $\rho=\rho_1$,

$(\delta f_{H_z})_{\rho=\rho_2}$ = frequency shift for conducting disk measuring H_z at $\rho=\rho_2$,

α = factor found from Figs. 6 and 7 in conjunction with (16) and the dimensions of the perturbing bodies.

It was found that the ratio E_z/Z_0H_z is approximately 1.3, which is in good agreement with a theoretical value of 1.25 from Fig. 3.

V. Periodic Disk Structure as Antenna

There is no radiation from points along the line unless the periodic structure is terminated, or any other discontinuity is introduced. The terminal plane may be treated as a radiating aperture with a field distribution $F(\rho, \phi)$. The radiation pattern is given by[11]

$$g(\theta, \phi') = (1 + \cos\theta) \int_0^{2\pi} \int_a^{\infty} F(\rho, \phi) \cdot e^{j(2\pi/\lambda_0)\rho \sin\theta \cos(\phi-\phi')} \rho d\rho d\phi \tag{18}$$

where $g(\theta, \phi')$ is the field intensity at a point on the surface of a sphere specified by the polar angles θ and ϕ'.

The calculation of radiation patterns follows closely the approach of Brown and Spector[4,6] to surface-wave end-fire antennas generally. It can be shown[6] that as the guided wavelength increases and approaches that of free space, an approximate expression for the radiation pattern is given by

$$g(\theta) = (1 + \cos\theta) \int_a^{\infty} \rho H_0(jk_0\rho) J_0\left(\frac{2\pi}{\lambda_0} \rho \sin\theta\right) d\rho. \tag{19}$$

This is a Lommel-type integral, and integration gives

$$g(\theta) = (1 + \cos\theta) \frac{k_0 a H_1(jk_0 a) J_0(u) + juH_0(jk_0 a) J_1(u)}{(k_0 a)^2 + u^2} \tag{20}$$

where

$$u = \frac{2\pi}{\lambda_0} a \sin\theta.$$

The expression in (20) can readily be evaluated with the help of tables. Values for half-amplitude beamwidths are given in Fig. 9 as functions of the disk diameter $2a/\lambda_0$, with spacing d as parameter. Values for k_0 in (20) have been obtained from Fig. 5(a). It is found that the beamwidth is reduced with decreasing diameter of the disks or increased spacing, both of which, in effect, produce a distribution of the guided wave over a larger aperture. It should be kept in mind, however, that the practicability of obtaining very narrow beams is dependent on the efficiency of exciting a pure surface wave with a guided wavelength nearly equal to free-space wavelength. Such a surface wave is very loosely bound to the surface, and the low efficiency of excitation gives rise to direct radiation from the antenna feed, with resulting broadening of the beam and unwanted sidelobes.

[11] S. Silver, "Microwave Antenna Theory and Design," McGraw-Hill Book Co., Inc., New York, N. Y.; 1949.

VI. Conclusions

A periodic structure consisting of a linear array of conducting disks has been investigated, both theoretically and experimentally. The resonator experiments have established the fact that nonradiating surface waves propagate along the structure. These are slow waves, that is, their phase velocity is less than the phase velocity of an electromagnetic wave in an unbounded medium.

The propagation constants for the "dipole mode" have been experimentally determined for structures of different dimensions. By using the radiating aperture approach, the beamwidth has been calculated when these periodic structures are used as end-fire antennas.

Exact expressions for the field have been set up. Subject to certain approximations, a secular equation has been derived from which the propagation constants may be calculated. Theoretical values are compared with experiments.

The purity of the "dipole mode" on the disk structure has been verified by means of perturbation experiments. The disk line has thus been found suitable for use as an end-fire antenna, provided the "dipole mode" is efficiently excited, without a great amount of direct radiation from the feeding end.

Acknowledgment

The author wishes to thank Prof. J. Brown, of University College, London, England, Prof. R. W. P. King and Dr. F. Hinchey of Harvard University, Cambridge, Mass., for many valuable discussions regarding this work.

The Sinusoidal Variation of Dissipation Along Uniform Waveguides*

GEORGE PERSKY†

Summary—**Standing waves in a waveguide with dielectric and/or metal wall losses generally give rise to expressions for power dissipation per unit length containing a term which is a sinusoidal function of the distance along the waveguide. In the present paper this phenomenon is explained and expressions for the dissipation are derived. The development is carried out for TE and TM modes in a uniform dielectric filled waveguide of arbitrary cross section, and then again from the standpoint of transmission line theory. The practical implications of the results are discussed.**

Introduction

When a standing wave exists in a lossy waveguide, the dissipation of power per unit length as a function of distance can generally be described by the sum of two terms, one of which is sinusoidal. While this fact has occasionally been recognized in one form or another,[1–3] it is commonly overlooked in practice, and no detailed treatment for the single mode case has, to the author's knowledge, been available. One can see intuitively that wall losses are greatest at the points of maximum magnetic field and dielectric losses at points of maximum electric field. Power attenuation in each traveling wave is therefore not proportional to $e^{\pm 2\alpha z}$ as is often assumed, and the improper use of such attenuation factors can lead to serious errors in the calculation of dissipation. This fact is not generally appreciated, although it is well known that in a dissipative guide it is not possible to speak of net power flow in terms of P_{inc} and P_{ref}, since these quantities are not well defined.

The purpose of this paper is to provide a firm basis for the accurate calculation of the distribution of dissipation along the direction of propagation and to point out the areas where calculations of this type are indicated.

Fig. 1 shows a section of uniform dielectric filled waveguide of arbitrary cross section with walls of surface resistivity r and filled with a dielectric material of conductivity σ. The dissipation in this waveguide will be found separately for the TE and TM mode cases. The analysis will be carried out in terms of normalized mode functions[4] (which, it is recognized,

* Received June 28, 1962; revised manuscript received, August 10, 1962. The work reported here was sponsored by the U. S. Army Signal Research and Development Laboratory, the Office of Naval Research and the Air Force Office of Scientific Research, under Contract AF-18(600)-1505.

† Microwave Research Institute, Polytechnic Institute of Brooklyn, Brooklyn, N. Y.

[1] W. K. Kahn, "A Theoretical and Experimental Investigation in Multimode Networks and Waveguide Transmission," Microwave Res. Inst., Polytechnic Inst. of Brooklyn, N. Y., Res. Rept. PIBMRI-818-60, pp. 79–86; September 21, 1960.

[2] D. D. King, "Measurements at Centimeter Wavelength," D. Van Nostrand Co., New York, N. Y., p. 27; 1952.

[3] R. W. P. King, "Transmission Line Theory," McGraw-Hill Book Co., Inc., New York, N. Y., p. 251; 1955.

[4] N. Marcuvitz, "Waveguide Handbook," McGraw-Hill Book Co., Inc., New York, N. Y., M.I.T. Rad. Lab. Ser., vol. 10; 1951.